SCIENTIFIC REP♥RTS

OPEN

Nuclear volume effects in equilibrium stable isotope fractionations of mercury, thallium and lead

Sha Yang[1,2] & Yun Liu[1]

The nuclear volume effects (NVEs) of Hg, Tl and Pb isotope systems are investigated with careful evaluation on quantum relativistic effects via the Dirac's formalism of full-electron wave function. Equilibrium $^{202}Hg/^{198}Hg$, $^{205}Tl/^{203}Tl$, $^{207}Pb/^{206}Pb$ and $^{208}Pb/^{206}Pb$ isotope fractionations are found can be up to 3.61‰, 2.54‰, 1.48‰ and 3.72‰ at room temperature, respectively, larger than fractionations predicted by classical mass-dependent isotope fractionations theory. Moreover, the NVE can cause mass-independent fractionations (MIF) for odd-mass isotopes and even-mass isotopes. The plot of $\Delta_{NV}^{199}Hg$ vs. $\Delta_{NV}^{201}Hg$ for Hg-bearing species falls into a straight line with the slope of 1.66, which is close to previous experimental results. For the first time, Pb^{4+}-bearing species are found can enrich heavier Pb isotopes than Pb^{2+}-bearing species to a surprising extent, e.g., the enrichment can be up to 4.34‰ in terms of $^{208}Pb/^{206}Pb$ at room temperature, due to their NVEs are in opposite directions. In contrast, fractionations among Pb^{2+}-bearing species are trivial. Therefore, the large Pb fractionation changes provide a potential new tracer for redox conditions in young and closed geologic systems. The magnitudes of NVE-driven even-mass MIFs of Pb isotopes (i.e., $\Delta_{NV}^{204}Pb$) and odd-mass MIFs (i.e., $\Delta_{NV}^{207}Pb$) are almost the same but with opposite signs.

With rapid progresses in mass-spectrometer, great interests on stable isotope fractionations of heavy elements have been aroused. Evidences showed that heavy elements could have surprising isotopic fractionations as the consequence of the NVE[1–9]. The NVE is originated from differences in nuclear size and nuclear shape of isotopes[2,10]. It doesn't belong to the well-known driving forces of equilibrium isotope fractionation, which are governed by the conventional Bigeleisen-Mayer theory[11] or Urey method[12].

The concept of NVE was proposed in spectrometric studies[10]. However, those early studies have not investigated its influences on isotopic fractionations. Fujii *et al.*[13] found anomalous isotope fractionations in uranium isotope exchange experiments which violated the Bigeleisen-Mayer equation (or Urey model) but suggested the cause to be the difference in nuclear spin. Nishizawa *et al.*[1] correctly interpreted the anomalous isotope effects of strontium by using isotope shift in atomic spectra (field shift). It was probably the first isotope NVE study. Hereafter, Bigeleisen[2] and Nomura *et al.*[3] independently recognized that those anomalous isotope fractionation phenomena, which were caused by the NVE, could lead to large stable isotope fractionations of heavy elements. Bigeleisen[2] accordingly added the NVE as an important contribution into a modified calculation formula of the equilibrium isotope fractionation factor. He pointed out that the NVE is only a second order correction in chemical bonds, which suggested the NVE can have minor effect on vibrational frequencies[14]. Importantly, he emphasized that the NVE can change isotopic fractionation largely alone via the change of ground-state electronic energy.

[1]State Key Laboratory of Ore Deposit Geochemistry, Institute of Geochemistry, Chinese Academy of Sciences, Guiyang 550002, China. [2]University of Chinese Academy of Sciences, Beijing 100049, China. Correspondence and requests for materials should be addressed to Y.L. (email: Liuyun@vip.gyig.ac.cn)
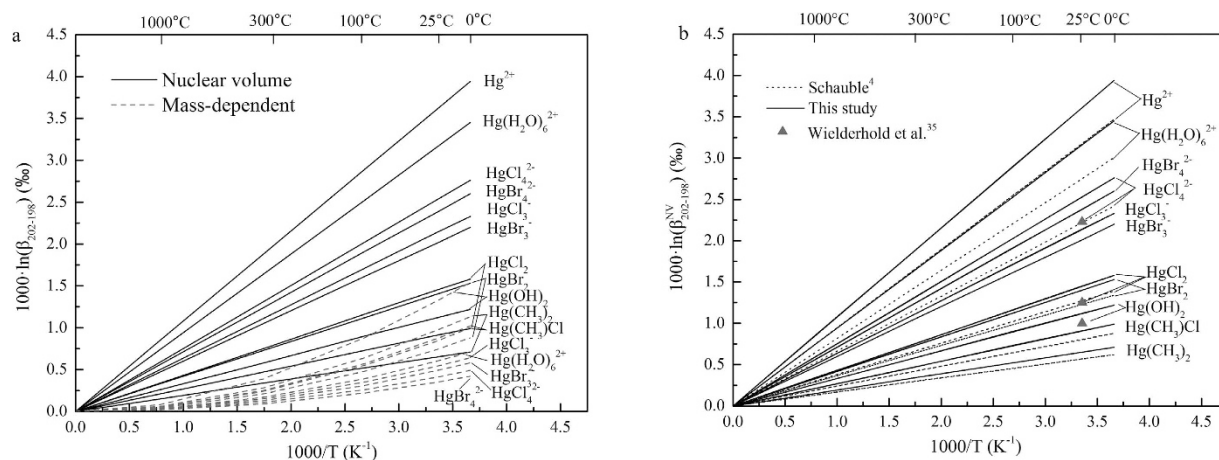
Figure 1. β-factors for Hg-bearing species relative to Hg⁰. (**a**) Contributions from CMDE and NVE, respectively. (**b**)Nuclear volume isotope fractionation factors ($\beta_{202-198}^{NV}$-factors relative to Hg⁰ vapor) compared to the results of Schauble[4] and Wielderhold et al.[35].

Toshiyuki Fujii and his co-workers have made tremendous efforts on experimental evaluations of NVEs for isotope systems, including Ti, Sn, Zr, Ni, Zn, Gd, Nd, Cr, Sr, Te and Cd etc.[15–29] Meanwhile, they performed quantum chemistry calculations for a few isotope systems, such as Zn[20,21], Ni[18], Tl[30] and Pb[31]. Schauble[4] used quantum chemistry methods to calculate NVEs of some heavy elements (e.g., Hg, Tl) and showed that the NVE could affect isotope fractionations of heavy elements to surprising degrees. Then, Abe et al.[5–7] independently calculated the NVE-driven fractionation factors of U-bearing species. Schauble[32] developed a new method to model nuclear volume effects in crystals. His new method was based on density functional theory (DFT), using the projector augmented wave method (DFT-PAW) with a three-dimensional periodic boundary condition for greater speed and compatibility.

In addition, Zheng et al.[33] and Ghosh et al.[34] did different experiments to estimate the NVE of mercury isotopes in the absence of light. They both assigned those mass-independent isotope fractionation signals as the consequence of the NVE. Wiederhold et al.[35] also did experimental and theoretical investigations on Hg mass-indpendent isotope fractionations. Schauble[4] and Wiederhold et al.[35] have explored small NVE-driven Hg isotope fractionations in organic Hg-bearing species in depth. Moynier et al.[9] reviewed the NVEs of Tl and U isotope systems in different natural environments, such as under low- or high-temperature conditions and in meteorites. The necessity of careful NVE evaluation during the exploration of new heavy elements is recognized by most people.

Right now, there are a few different computational methods used to investigate quantum relatistic effects associated with the NVE, e.g., Schauble[4,32] used the DIRAC and ABINIT software package, Abe et al.[5–7] used a four-component relativistic atomic program package-GRASP2K, Fujii et al.[18,20,21,30,31] used a software provided by Tokyo University (UTchem). Recently, Nemoto et al.[36] found a two-component realtivistic method (the finite-order Douglas-Kroll-Hess method with infinite-order spin-orbit interactions for the one-electron term and atomic-mean-field spin-same-orbit interaction for the two-electron term, i.e., IODKH-IOSO-MFSO) with almost equivalent accuracy but 30 times faster than the previous four-component method by DIRAC software package. They also predicted the IODKH-IOSO-MFSO method could compute larger system for future NVE calculation.

Here we calculate the NVE-driven fractionation factors of Hg-, Tl- and Pb-bearing species by using full-electron quantum chemistry calculation methods. Our method is similar to that of Schauble[4], in which quantum relativistic effects have been carefully evaluated via four-component Dirac equation formalism[37,38]. Not only more new Hg- and Pb-bearing species (e.g., $HgBr_4^{2-}$, $HgCl_3^{-}$, $HgBr_3^{-}$ and many Pb^{4+}-bearing species) are calculated here, but more mass-independent fractionations are investigated in light of recent findings on even-number Hg isotope MIFs[39,40]. Large fractionations (up to ca. 4‰ at room temperature) between Pb^{4+}- and Pb^{2+}-bearing species are found for the first time.

Results

Equilibrium stable isotope fractionations of Hg-, Tl-, and Pb-bearing species are shown in Figures 1, 2, and 3 and Tables 1, 2, and 3 relative to Hg⁰, Tl⁰, and Pb⁰ in terms of $1000 \cdot \ln\beta$, including conventional mass-dependent ($1000 \cdot \ln\beta^{MD}$) and nuclear volume effect fractionation factors ($1000 \cdot \ln\beta^{NV}$).

Hg isotope system. NVEs alone can fractionate ²⁰²Hg/¹⁹⁸Hg isotopes up to 3.61‰ at 25 °C. However, the largest classical mass-dependent fractionation are only 1.32‰ for ²⁰²Hg/¹⁹⁸Hg at 25 °C. All Hg-bearing species enrich heavier isotope (²⁰²Hg) relative to Hg⁰ vapor. The NVE-driven isotope fractionations of inorganic species, such as Hg^{2+}, $HgCl_4^{2-}$, $HgBr_4^{2-}$, $HgCl_3^{-}$, $HgBr_3^{-}$, $HgCl_2$, $HgBr_2$, $Hg(H_2O)_6^{2+}$ or
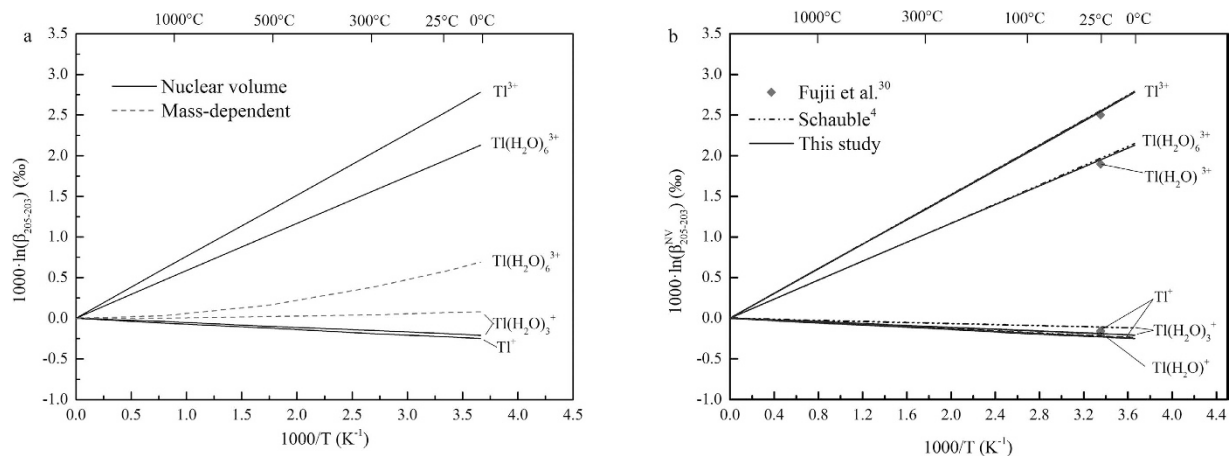
Figure 2. β-factors for Tl-bearing species relative to Tl⁰. (**a**) Contributions from CMDE and NVE, respectively. (**b**) Nuclear volume isotope fractionation factors ($\beta_{205-203}^{NV}$-factors relative to Tl^0) compared to the results of Schauble[4] and Fujii *et al.*[30].
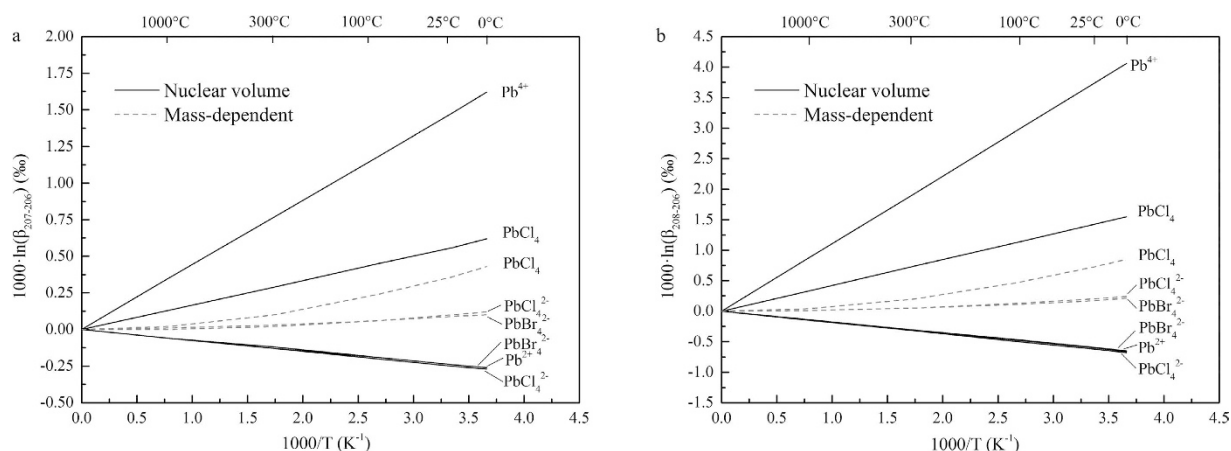

Figure 3. β-factors for Pb-bearing species relative to Pb⁰, including CMDE and NVE. (**a**) $\beta_{208-206}$-factors of $^{207}Pb/^{206}Pb$. (**b**) $\beta_{208-206}$-factors of $^{208}Pb/^{206}Pb$.

$Hg(OH)_2$, are larger than those of organic molecules (e.g., $Hg(CH_3)Cl$ and $Hg(CH_3)_2$). On the contrary, CMDE fractionations of inorganic species are smaller than organic compounds except for $Hg(OH)_2$.

Tl isotope system. The NVE-driven fractionation of $^{205}Tl/^{203}Tl$ isotopes is up to 2.54‰ relative to Tl^0 and the CMDE is only 0.58‰ for $Tl(H_2O)_6^{3+}$ and 0.07‰ for $Tl(H_2O)_3^{+}$ at 25 °C. Our NVE results show that Tl^{3+} ion and Tl^{3+}-bearing compounds enriches heavier isotope (^{205}Tl) relative to Tl^0. However, Tl^+ ion and Tl^+-bearing compounds enriches lighter isotope (^{203}Tl) compared to Tl^0. Note that β-values of Tl^+-bearing species are even smaller than the unity. This is because NVE tends to let heavier isotopes to be enriched in those atoms or ions with fewer s electrons or with more p, d and f electrons. Tl^0 has more p electrons than Tl^+-bearing species does.

Pb isotope system. NVEs induce Pb isotope fractionations up to 1.48‰ ($^{207}Pb/^{206}Pb$) and 3.72‰ ($^{208}Pb/^{206}Pb$) relative to Pb^0, at 25 °C. However, contributions from classical mass-dependent fractionation are small, about 0.1–0.4‰ for $^{207}Pb/^{206}Pb$ and 0–2–0.7‰ for $^{208}Pb/^{206}Pb$ at 25 °C. The isotope fractionations of Pb^{4+}-bearing species (e.g., $PbCl_4$) are larger than those of Pb^{2+}-bearing species (e.g., $PbCl_4^{2-}$ or $PbBr_4^{2-}$) in terms of NVE or CMDE.

Mass-independent fractionation of Hg and Pb isotopes. Table 4 shows NVE-driven mass-independent fractionations for ^{199}Hg, ^{200}Hg, and ^{201}Hg isotopes at room temperature. Those MIFs are relative to the MIF of Hg vapor (i.e., Hg^0). If the real MIF value of a specific Hg-bearing species is needed, one needs convert the number listed in Table 4 via the aid of experimental MIF data of Hg vapor.

	This study[a]					Schauble[b]					Wiederhold et al.[c]
	0°C	25°C	100°C	300°C	1000°C	0°C	25°C	100°C	300°C	1000°C	25°C
CMDE fractionation factor ($1000 \cdot \ln \beta^{MD}_{202-198}$)											
Hg^0	0	0	0	0	0	0	0	0	0	0	
Hg^{2+}	0	0	0	0	0	0	0	0	0	0	
$HgCl_2$	1.00	0.84	0.55	0.24	0.05	1.08	0.92 ± 0.1	0.60	0.26	0.05	0.84
$HgBr_2$	0.88	0.74	0.48	0.21	0.04	0.95	0.80 ± 0.1	0.51	0.22	0.04	
$Hg(CH_3)Cl$	1.02	0.87	0.57	0.25	0.05	1.04	0.89 ± 0.1	0.58	0.25	0.05	
$Hg(CH_3)_2$	1.13	0.97	0.64	0.28	0.06	1.14	0.97 ± 0.1	0.65	0.29	0.06	
$HgCl_3^-$	0.64	0.54	0.35	0.15	0.03						
$HgCl_4^{2-}$	0.49	0.41	0.26	0.11	0.02	0.67	$0.56+0.7/-0.1$	0.36	0.15	0.03	0.40
$HgBr_3^-$	0.58	0.49	0.31	0.13	0.03						
$HgBr_4^{2-}$	0.42	0.35	0.22	0.09	0.02						
$Hg(H_2O)_6^{2+}$	0.71	0.60	0.39	0.17	0.03	1.13	0.96 ± 0.4	0.62	0.27	0.05	
$Hg(OH)_2$	1.54	1.32	0.88	0.39	0.08						1.19
NVE fractionation factor ($1000 \cdot \ln \beta^{NV}_{202-198}$)											
Hg^0	0	0	0	0	0	0	0	0	0	0	
Hg^{2+}	3.94	3.61	2.89	1.88	0.85	3.47	3.17 ± 0.6	2.54	1.65	0.74	
$HgCl_2$	1.58	1.45	1.16	0.75	0.34	1.39	1.27 ± 0.3	1.02	0.66	0.30	1.25
$HgBr_2$	1.53	1.40	1.12	0.73	0.33	1.34	1.23 ± 0.2	0.98	0.64	0.29	
$Hg(CH_3)Cl$	0.99	0.91	0.73	0.47	0.21	0.88	0.80 ± 0.2	0.64	0.42	0.19	
$Hg(CH_3)_2$	0.71	0.65	0.52	0.34	0.15	0.62	0.57 ± 0.1	0.45	0.30	0.13	
$HgCl_3^-$	2.33	2.14	1.71	1.11	0.50						
$HgCl_4^{2-}$	2.76	2.53	2.02	1.31	0.59	2.42	2.22 ± 0.4	1.77	1.16	0.52	2.23
$HgBr_3^-$	2.20	2.01	1.61	1.05	0.47						
$HgBr_4^{2-}$	2.60	2.38	1.91	1.24	0.56						
$Hg(H_2O)_6^{2+}$	3.45	3.16	2.52	1.64	0.74	3.01	2.75 ± 0.6	2.20	1.43	0.64	
$Hg(OH)_2$	1.22	1.12	0.90	0.58	0.26						1.00
Total fractionation factor ($1000 \cdot \ln \beta_{202-198}$)											
Hg^0	0	0	0	0	0	0	0	0	0	0	
Hg^{2+}	3.94	3.61	2.89	1.88	0.85	3.47	3.17 ± 0.6	2.54	1.65	0.74	
$HgCl_2$	2.58	2.29	1.71	0.99	0.39	2.47	2.19 ± 0.3	1.62	0.92	0.35	2.09
$HgBr_2$	2.41	2.14	1.60	0.94	0.37	2.29	2.03 ± 0.2	1.49	0.86	0.33	
$Hg(CH_3)Cl$	2.01	1.78	1.30	0.72	0.26	1.92	1.69 ± 0.2	1.22	0.67	0.24	
$Hg(CH_3)_2$	1.84	1.62	1.16	0.62	0.21	1.76	1.54 ± 0.1	1.10	0.59	0.19	
$HgCl_3^-$	2.97	2.68	2.06	1.26	0.53						
$HgCl_4^{2-}$	3.25	2.94	2.28	1.42	0.61	3.09	$2.78+0.8/0.4$	2.13	1.31	0.55	2.63
$HgBr_3^-$	2.78	2.50	1.92	1.18	0.50						
$HgBr_4^{2-}$	3.02	2.73	2.13	1.33	0.58						
$Hg(H_2O)_6^{2+}$	4.16	3.76	2.91	1.81	0.77	4.14	3.71 ± 0.7	2.82	1.70	0.69	
$Hg(OH)_2$	2.76	2.44	1.78	0.97	0.34						2.19

Table 1. Calculated stable isotope fractionation factors for Hg-bearing species relative to Hg^0 (in per mil), including conventional mass-dependent effect (CMDE) fractionation factors ($1000 \cdot \ln \beta^{MD}_{202-198}$) and nuclear volume effect (NVE) fractionation factors ($1000 \cdot \ln \beta^{NV}_{202-198}$). [a]Calculated with $<r^2>$ values of Fricke and Heilig[41] by using the software package DIRAC13.1. [b]Calculated with $<r^2>$ values of Angeli[42] by using the software package DIRAC04 by Schauble[4]. [c]Calculated with $<r^2>$ values of Fricke and Heilig[41] by using the software package DIRAC08 by Wiederhold et al.[35].

	This study					Schauble[a])					Fujii et al.[b])
	0°C	25°C	100°C	300°C	1000°C	0°C	25°C	100°C	300°C	1000°C	25°C
CMDE fractionation factor ($1000 \cdot \ln\ \beta^{MD}_{205-203}$)											
Tl^0	0	0	0	0	0	0	0	0	0	0	
Tl^+	0	0	0	0	0	0	0	0	0	0	
Tl^{3+}	0	0	0	0	0	0	0	0	0	0	
$Tl(H_2O)_3^+$	0.08	0.07	0.04	0.02	0.00	0.08	0.07 ± 0.1	0.04	0.02	0.00	0.063[c])
$Tl(H_2O)_6^{3+}$	0.69	0.58	0.38	0.16	0.03	0.77	0.65 ± 0.2	0.44	0.18	0.04	0.423
NVE fractionation factor ($1000 \cdot \ln\ \beta^{NV}_{205-203}$)											
Tl^0	0	0	0	0	0	0	0	0	0	0	
Tl^+	−0.25	−0.23	−0.19	−0.12	−0.06	−0.24	-0.22 ± 0.04	−0.18	−0.11	−0.05	−0.157
Tl^{3+}	2.78	2.54	2.03	1.32	0.60	2.79	2.55 ± 0.5	2.04	1.32	0.60	2.501
$Tl(H_2O)_3^+$	−0.21	−0.19	−0.15	−0.10	−0.04	−0.12	-0.11 ± 0.02	−0.09	−0.06	−0.03	−0.168[d])
$Tl(H_2O)_6^{3+}$	2.13	1.95	1.56	1.02	0.46	2.15	1.97 ± 0.4	1.57	1.02	0.46	1.898[e])
Total fractionation factor ($1000 \cdot \ln\ \beta_{205-203}$)											
Tl^0	0	0	0	0	0	0	0	0	0	0	
Tl^+	−0.25	−0.23	−0.19	−0.12	−0.06	−0.24	-0.22 ± 0.04	−0.18	−0.11	−0.05	
Tl^{3+}	2.78	2.54	2.03	1.32	0.60	2.79	2.55 ± 0.5	2.04	1.32	0.60	
$Tl(H_2O)_3^+$	−0.13	−0.12	−0.11	−0.08	−0.04	−0.04	-0.04 ± 0.1	−0.05	−0.04	−0.03	
$Tl(H_2O)_6^{3+}$	2.82	2.53	1.94	1.18	0.49	2.92	2.62 ± 0.4	2.01	1.20	0.50	

Table 2. Calculated stable isotope fractionation factors for Tl^0 (in per mil), including conventional mass-dependent effect (CMDE) fractionation factors ($1000 \cdot \ln\ \beta^{MD}_{205-203}$) and nuclear volume effect (NVE) fractionation factors ($1000 \cdot \ln\ \beta^{NV}_{205-203}$). [a]Calculated by Schauble[4] using the software package DIRAC04. [b]Calculated by Fujii et al.[30] using UTChem program at 298 K. [c]Calculated for $Tl(H_2O)_6^+$. [d]Calculated for $Tl(H_2O)^+$. [e]Calculated for $Tl(H_2O)^{3+}$.

For example, according to Ghosh et al.[34], the NVE-driven $\Delta^{199}_{NV}Hg$ of Hg^0 is about 0.14‰, therefore, $\Delta^{199}_{NV}Hg$ of Hg^{2+} should be −0.59‰ (i.e., −0.73‰ of Hg^{2+} listed in Table 4 plus 0.14‰).

All $\Delta^{199}_{NV}Hg$ and $\Delta^{201}_{NV}Hg$ values listed in Table 4 except for Hg^0 are negative. For all studied Hg species, the MIF ratio of two odd-mass isotopes (i.e., $\Delta^{199}_{NV}Hg/\Delta^{201}_{NV}Hg$) will fall on a straight line with the slope of 1.66 (Fig. 4), suggesting they will be changed in a proportional way. This result is almost identical to a previous theoretical result[35] (i.e., with the slope of 1.65). This special relationship can be used to study MIFs caused by other reason via distinguishing the NVE signals from them.

Moreover, NVE can also cause mass-independent fractionations for odd-mass isotope (^{207}Pb) and even-mass isotope (^{204}Pb) (Table 5). The largest signals of NVE-driven MIF are up to −0.39‰ ($\Delta^{207}_{NV}Pb$) and 0.41‰ ($\Delta^{204}_{NV}Pb$) among all the studied species relative to Pb^0 at 25°C. The signs of even-mass isotope MIF ($\Delta^{204}_{NV}Pb$) and odd-mass isotope MIF ($\Delta^{207}_{NV}Pb$) are opposite to each other although their magnitudes are almost the same (Table 5).

The calculation details, including optimized geometries, energies, harmonic vibrational frequencies, et al., have been documented in the Supplementary file for interested reader.

Discussion

One of the special features of NVE is that it can cause large isotope fractionations between isolated atoms and ions (e.g., Hg^{2+}-Hg^0, Tl^{3+}-Tl^+ and Pb^{4+}-Pb^{2+}), which there would be no fractionation at all if based on the classical mass-dependent isotope fractionation theory, because there is no difference in terms of kinetic energies for them. Moreover, it seems that ions with more extra charges (e.g., with fewer s orbital electrons) can have larger NVEs and isotope fractionation potential than those with lesser charges (e.g., Tl^{3+} vs. Tl^+, Pb^{4+} vs. Pb^{2+}).

Comparing with previous studies (Fig. 1b and Table 1), our NVE-driven Hg isotope fractionation results are noticeably different from those of Schauble[4] and Wiederhold et al.[35]. The NVE is proportional to difference in mean square nuclear charge radius of different nuclei (i.e., $NVE \propto \delta<r^2>$ and $\delta<r^2> = <r^2>_A - <r^2>_{A'}$), as King[10] has pointed out based on spectrometric results. Therefore, we can explain the difference between Schauble[4] and our results very clearly. Schauble[4] used the nuclear charge radii of Angeli[42] (i.e., $<r^2>^{1/2}$ of ^{202}Hg and ^{198}Hg are 5.4633fm and 5.4466fm) and the nuclear charge radius difference ($\delta<r^2> = <r^2>_A - <r^2>_{A'}$) is 0.182fm². But we use the nuclear charge radii from

species	0°C	25°C	100°C	300°C	1000°C	0°C	25°C	100°C	300°C	1000°C
	CMDE fractionation factor ($1000 \cdot \ln \beta^{MD}_{207-206}$)					CMDE fractionation factor ($1000 \cdot \ln \beta^{MD}_{208-206}$)				
Pb^0	0	0	0	0	0	0	0	0	0	0
Pb^{2+}	0	0	0	0	0	0	0	0	0	0
Pb^{4+}	0	0	0	0	0	0	0	0	0	0
$PbCl_4^{2-}$	0.12	0.10	0.06	0.03	0.01	0.24	0.20	0.13	0.05	0.01
$PbBr_4^{2-}$	0.10	0.09	0.06	0.02	0.00	0.21	0.17	0.11	0.05	0.01
$PbCl_4$	0.43	0.36	0.24	0.10	0.02	0.85	0.72	0.47	0.20	0.04
	NVE fractionation factor ($1000 \cdot \ln \beta^{NV}_{207-206}$)					NVE fractionation factor ($1000 \cdot \ln \beta^{NV}_{208-206}$)				
Pb^0	0	0	0	0	0	0	0	0	0	0
Pb^{2+}	−0.26	−0.24	−0.19	−0.13	−0.06	−0.66	−0.60	−0.48	−0.31	−0.14
Pb^{4+}	1.61	1.48	1.18	0.77	0.35	4.06	3.72	2.97	1.93	0.87
$PbCl_4^{2-}$	−0.27	−0.25	−0.20	−0.13	−0.06	−0.68	−0.62	−0.50	−0.32	−0.15
$PbBr_4^{2-}$	−0.26	−0.24	−0.19	−0.12	−0.06	−0.65	−0.59	−0.47	−0.31	−0.14
$PbCl_4$	0.62	0.56	0.45	0.29	0.13	1.55	1.42	1.13	0.74	0.33
	Total fractionation factor ($1000 \cdot \ln \beta_{207-206}$)					Total fractionation factor ($1000 \cdot \ln \beta_{208-206}$)				
Pb^0	0	0	0	0	0	0	0	0	0	0
Pb^{2+}	−0.26	−0.24	−0.19	−0.13	−0.06	−0.66	−0.60	−0.48	−0.31	−0.14
Pb^{4+}	1.61	1.48	1.18	0.77	0.35	4.06	3.72	2.97	1.93	0.87
$PbCl_4^{2-}$	−0.15	−0.15	−0.14	−0.10	−0.05	−0.44	−0.42	−0.37	−0.27	−0.14
$PbBr_4^{2-}$	−0.16	−0.15	−0.13	−0.10	−0.06	−0.44	−0.42	−0.36	−0.26	−0.13
$PbCl_4$	1.05	0.92	0.69	0.39	0.15	2.40	2.14	1.60	0.94	0.37

Table 3. Calculated stable isotope fractionation factors for Pb-bearing species relative to Pb^0 (in per mil), including conventional mass-dependent effect (CMDE) and nuclear volume effect (NVE).

	$^{198}Hg/^{198}Hg$	$^{199}Hg/^{198}Hg$	$^{200}Hg/^{198}Hg$	$^{201}Hg/^{198}Hg$	$^{202}Hg/^{198}Hg$
NV scaling factor	**0.0**	**0.0525**	**0.4732**	**0.6312**	**1.0**
CMD scaling factor	**0.0**	**0.2539**	**0.5049**	**0.7539**	**1.0**
	$\Delta^{198}_{NV}Hg$	$\Delta^{199}_{NV}Hg$	$\Delta^{200}_{NV}Hg$	$\Delta^{201}_{NV}Hg$	$\Delta^{202}_{NV}Hg$
Hg^0	0.0	0.0	0.0	0.0	0.0
Hg^{2+}	0.0	−0.73	−0.11	−0.44	0.0
$HgCl_2$	0.0	−0.29	−0.05	−0.18	0.0
$HgBr_2$	0.0	−0.28	−0.04	−0.17	0.0
$Hg(CH_3)Cl$	0.0	−0.18	−0.03	−0.11	0.0
$Hg(CH_3)_2$	0.0	−0.13	−0.02	−0.08	0.0
$HgCl_3^-$	0.0	−0.43	−0.07	−0.26	0.0
$HgCl_4^{2-}$	0.0	−0.51	−0.08	−0.31	0.0
$HgBr_3^-$	0.0	−0.40	−0.06	−0.25	0.0
$HgBr_4^{2-}$	0.0	−0.48	−0.08	−0.29	0.0
$Hg(H_2O)_6^{2+}$	0.0	−0.64	−0.10	−0.39	0.0
$Hg(OH)_2$	0.0	−0.23	−0.04	−0.14	0.0

Table 4. Conventional mass-dependent (CMD) and nuclear volume (NV) scaling factors and $\Delta^A_{NV}Hg$ values for different Hg-bearing species relative to Hg^0 at 25°C.

Fricke and Heilig[41] (i.e., $<r^2>^{1/2}$ of ^{202}Hg and ^{198}Hg are 5.462fm and 5.443fm) and the nuclear charge radius difference ($\delta<r^2> = <r^2>_A - <r^2>_{A'}$) is 0.207fm². Our results are roughly 1.137 times of those of Schauble[4], consistent with the radii difference ratio, i.e., 0.207/0.182 = 1.137.
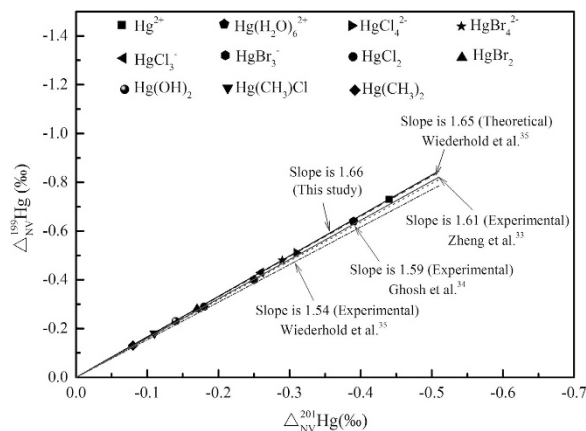
Figure 4. Δ_{NV}^{199}Hg versus Δ_{NV}^{201}Hg from NVE (Δ_{NV}^{A}Hg-factors relative to Hg^0 vapor) for Hg-bearing species at 25 °C. The black line is the slope of Δ^{199}Hg/Δ^{201}Hg of this study. The gray dash, dark gray solid, dark gray dot, dark gray short dash dot lines are the slop of Δ^{199}Hg/Δ^{201}Hg based on theoretical NVE-driven MIF calculated with radii of Landolt-Boernstein Databas[41] (calculated by Wiederhold et al.[35]), experimental NVE-driven MIF of Zheng et al.[33], Ghosh et al.[34], Wiederhold et al.[35], respectively.

	$^{204}Pb/^{206}Pb$	$^{206}Pb/^{206}Pb$	$^{207}Pb/^{206}Pb$	$^{208}Pb/^{206}Pb$
NV scaling factor	−0.9097	0.0	0.3980	1.0
CMD scaling factor	−1.0193	0.0	0.5026	1.0
	$\Delta_{NV}^{204}Pb$	$\Delta_{NV}^{206}Pb$	$\Delta_{NV}^{207}Pb$	$\Delta_{NV}^{208}Pb$
Pb^0	0.0	0.0	0.0	0.0
Pb^{2+}	−0.07	0.0	0.06	0.0
Pb^{4+}	0.41	0.0	−0.39	0.0
$PbCl_4^{2-}$	−0.07	0.0	0.06	0.0
$PbBr_4^{2-}$	−0.06	0.0	0.06	0.0
$PbCl_4$	0.16	0.0	−0.15	0.0

Table 5. Conventional mass-dependent (CMD) and nuclear volume (NV) scaling factors and Δ_{NV}^{A}Pb values for different Pb-bearing species relative to Pb^0 at 25 °C.

We use the same mean square nuclare radii as Wiederhold et al.[35], but different methods (i.e., DHF vs. MP2, respectively), which lead to different results. In addition, there are suggestions that calculated results of Hg-bearing species used the mean square nuclear charge radii of Fricke and Heilig[41] are closer to the experiment results[35]. Note that different versions of the calculation software package (i.e., DIRAC04 and DIRAC13.1) have little impact on the calculated results (see Table S6).

Our NVE-driven Tl isotope fractionation results are in comparison with those of Schauble[4] and Fujii et al.[30] in terms of $1000 \cdot \ln\beta^{NV}$ (Fig. 2b and Table 2). Our results agree with those of Schauble[4] perfectly because of using the similar methods and the same mean square nuclear charge radii (i.e., those radii from Angeli[42]). The only one exception is for the $Tl(H_2O)_3^+$ case. The fractionations between $Tl(H_2O)_3^+$ and Tl^0 are larger than those of Schabule[4], i.e., our result is −0.19‰ and their result is −0.11‰, at 25 °C. Our results are indeed very close to those of Fujii et al.[30] with small differences (ca. 0.04–0.07‰).

Previous researches have shown mercury can undergo mass-dependent fractionation (MDF) as well as mass-independent fractionation (MIF) for odd-mass isotopes (Δ^{199}Hg or Δ^{201}Hg)[43–46] and even-mass isotope (Δ^{200}Hg)[39,40]. The mechanism leading to the even-number Hg isotope mass-independent fractionation is still unclear.

Gratz et al.[39] firstly reported Δ^{200}Hg in Great Lakes precipitation and ambient air up to 0.25‰. Later, Chen et al.[40] found larger Δ^{200}Hg in precipitation from Peterborough where is located in subarctic zone. They showed that snow samples obtained in winter have surprisingly large Δ^{200}Hg values (up to 1.24‰) and rain water obtained in other seasons has much smaller Δ^{200}Hg values (about 0.21‰ ~ 0.42‰). However, there is no convincing evidence can explain the even-mass number Hg MIF enigma.

With the calculation data from this study, we find that the NVE-driven $\Delta_{NV}^{200}Hg$ cannot be the reason to explain those even-mass number Hg MIF results. First, the magnitudes of NVE-driven $\Delta_{NV}^{200}Hg$ are much smaller than those found by Gratz et al.[39] and Chen et al.[40]. Second, the sign of NVE-driven even-mass number Hg MIFs calculated here is opposite to those reported $\Delta^{200}Hg$ results, meaning the NVE causes depletion of ^{200}Hg instead of enrichment of ^{200}Hg relative to ^{198}Hg. Therefore, the observed large positive $\Delta^{200}Hg$ signals must have other reasons or processes to be produced.

Because the half-life times of uranium isotopes are all very long, e.g., 4.5Ga for ^{238}U and 0.7Ga for ^{235}U, people actually treat uranium isotope system as a stable one in many young geologic systems[47,48]. As the decayed products of uranium, Pb isotope system can also be treated as a regular stable isotope system for young and closed geologic systems with homogenized formation processes. For example, in some rocks formed less than 10 million years (or younger), or in some plants, or in any system which is young and homogenized before its formation. The equilibrium Pb isotope fractionations between two compounds in such systems can be meaningful and useful. In such systems, the radiogenic Pb isotope differences are no longer existing but homogenized to a background value. For instance, a system with inherited very high $^{208/206}Pb$ value has been homogenized in some processes. The compounds in such system will all have very high $^{208/206}Pb$ values. Meanwhile, the small differences of $^{208/206}Pb$ values among different compounds are caused by mass-driven and NVE-driven isotope fractionations. Our results can be used to explain such differences.

Fujii et al.[31] firstly reported calculated NVE-driven Pb isotope fractionation factors for Pb^0 and Pb^{2+}-bearing species. We provide results of several new Pb-bearing species especially for Pb^{4+}-bearing species. If comparing the NVE results between Pb^0 and Pb^{2+} of Fujii et al.[31] and ours, our results are marginally larger than theirs ($^{208}Pb/^{206}Pb$: 0.60‰ vs. 0.393‰ and $^{207}Pb/^{206}Pb$: 0.24‰ vs. 0.156‰) due to different methods and software packages used. In general, Pb isotope fractionations among Pb^{2+}-species are very small even with the driving force of NVE. However, we find surprisingly large fractionations (ca. 2 to 4‰) between Pb^{4+}-bearing species and Pb^{2+}-bearing species at room temperature. The fractionation magnitudes are similar or even larger than those Fe isotope fractionations between ferric and ferrous Fe-bearing species (e.g., $Fe^{3+}_{(aq)}$ vs. $Fe^{2+}_{(aq)}$) at low temperature, which have been broadly used as tracer for the change of redox conditions. Therefore, Pb isotope fractionations probably can also be used as a new tracer to study redox condition changes in young and closed geologic systems.

The occurrence of such large isotope fractionations is because the β-values of Pb^{4+}-bearing and Pb^{2+}-bearing species are in different directions, as the consequence of unique nuclear volume effects. Pb^{4+}-bearing species enrich heavy isotopes relative to Pb^0. However, Pb^{2+}-bearing species enrich light isotope compared to Pb^0, meaning β-values of Pb^{2+}-bearing species are smaller than the unity. It is similar to the case of Tl^+-bearing species. Pb^0 is the one has more p electrons than Pb^{2+}-bearing species. This finding cannot be explained if only based on classical isotope fractionation theory, which suggests all β values of any kind of isotope systems must be equal or larger than the unity.

Conclusions

In this study, quantum chemical calculations (Dirac-Hartree-Fock) confirm that the nuclear volume effect plays a dominant role in equilibrium isotope fractionation for mercury, thallium and lead systems compared to the contributions of conventional mass-dependent effect, and agree with those conclusions of previous studies[4,30,31]. NVE-driven $^{202}Hg/^{198}Hg$, $^{205}Tl/^{203}Tl$, $^{207}Pb/^{206}Pb$ and $^{208}Pb/^{206}Pb$ fractionations for Hg-, Tl- and Pb-bearing species can be up to 3.61‰, 2.54‰, 1.48‰ and 3.72‰ at 25 °C, respectively. Moreover, the NVE-driven mass-independent fractionations of ^{199}Hg are larger than those of ^{201}Hg and ^{200}Hg which is up to -0.73‰. The ratio of $\Delta_{NV}^{199}Hg/\Delta_{NV}^{201}Hg$ is 1.66 which agrees well with previous experimental and theoretical results. Furthermore, those NVE-driven MIFs of ^{200}Hg calculated here are not only too small to be compared with the $\Delta^{200}Hg$ results reported in snow and water samples[39,40], but also with the opposite sign, meaning the NVE is not the reason of those $\Delta^{200}Hg$ signals.

Surprisingly, we find Pb isotope fractionations between Pb^{4+}-bearing and Pb^{2+}-bearing species can be up to 2 - 4‰ at room temperatures, suggesting a potential new tracer for redox condition changes in young and closed geologic systems. The NVE-driven MIFs of $\Delta_{NV}^{207}Pb$ and $\Delta_{NV}^{204}Pb$ are with moderate magnitudes but in opposite signs (i.e., $\Delta_{NV}^{207}Pb \approx -\Delta_{NV}^{204}Pb$).

Methods

Conventional mass-dependent effect (CMDE). Bigeleisen and Mayer[11] and Urey[12] suggested a well-known method for calculating the isotope fractionation factor, which is called the Bigeleisen-Mayer equation (hereafter B-M equation) or the Urey model. The B-M equation was based on the Born-Oppenheimer and harmonic approximations. According to the B-M equation, the natural logarithm of the isotope fractionation factor for an isotope exchange reaction under high-temperature approximations is

$$\varepsilon \approx \ln \alpha_0 \propto \Delta m/(mm'T^2) \qquad (1)$$

where ε is the isotope enrichment factor and is roughly equal to $\ln \alpha_0$; α_0 is the isotope fractionation factor; m and m′ are the masses of the heavy and light isotopes, respectively; Δm is the relative mass

difference of isotopes (i.e., $\Delta m = m - m'$). When the temperature is constant, enrichment factor is proportional to $\Delta m/mm'$. According to this equation, the isotope fractionation of heavy elements (e.g., Hg, Tl or Pb) would be small.

For an exchange reaction $A'Y + AX = A'X + AY$, the equilibrium CMDE fractionation factors is calculated[11,12]

$$\alpha^{CMDE} = RPFR\left(\frac{AY}{A'Y}\right)/RPFR\left(\frac{AX}{A'X}\right) \tag{2}$$

where RPFR is the reduced partition function ratio and it is expressed in term of the harmonic vibrational frequencies with isotope substitution

$$RPFR = \prod_{i}^{3n-6} \frac{u_i(A'X)}{u_i(AX)} \frac{\exp(-u_i(A'X)/2)}{\exp(-u_i(AX)/2)} \frac{1-e^{-u_i(AX)}}{1-e^{-u_i(A'X)}} \tag{3}$$

where A and A' are the heavy and light isotopes of the element A; $u_i(AX) = h\nu_i(AX)/kT$; $\nu_i(AX)$ is the ith harmonic vibrational frequency of AX molecule; h and k are Planck and Boltzmann constant; T is the absolute temperature.

Nuclear volume effect (NVE).

Based on spectrometric results, King[10] proposed that the NVE was proportional to difference in mean square nuclear charge radius of different nuclei (i.e., $NVE \propto \delta<r^2>$ and $\delta<r^2> = <r^2>_A - <r^2>_{A'}$). Upon the inspiration of U isotope exchange experiments, Bigeleisen[2] revised the B-M equation and added the NVE term into it. The logarithm of the corrected isotope fractionation factor became

$$\varepsilon \approx \ln \alpha = \ln \alpha_0 + \ln K_{anh} + \ln K_{BOELE} + \ln K_{fs} + \ln K_{hf} \tag{4}$$

where $\ln\alpha_0$ is the isotope fractionation factor under the B-M equation approximations; $\ln K_{anh}$ is the anharmonic correction term; $\ln K_{BOELE}$ is the correction to the Born-Oppenheimer approximation; $\ln K_{fs}$ is the NVE term (also called nuclear field shift); $\ln K_{hf}$ is the term for nuclear spin effect. In the terminology of Bigeleisen, the nuclear field shift actually includes both shape and size effects. However, the contribution from nuclear size is easy to calculate but that from nuclear shape is very difficult to evaluate and trivial. Therefore, people trend to use NVE instead of nuclear field shift for more precise description[4].

Because of extremely small anharmonic corrections for heavy elements, $\ln K_{anh}$ can be safely neglected[2]. The correction to the Born-Oppenheimer approximation is related to $\Delta m/mm'$[49,50]. Therefore, $\ln\alpha_0$ and $\ln K_{BOELE}$ are both proportional to $\Delta m/mm'$ when temperature is a constant. Based on the investigations on U isotope exchange reactions, Bigeleisen[2] showed that nuclear spin effect was also very small and could be safely neglected.

Because the NVE is related to the difference in ground-state electronic energies, it can be written as[2]

$$\ln K_{fs} = (kT)^{-1}\{[E^0(AX) - E^0(A'X)] - E^0(AY) - E^0(A'Y)]\} \tag{5}$$

where E^0 is the ground-state electronic energy; AX and A'X represent different isotopologues; k is the Boltzmann's constant and T is in absolute temperature (K). We can see the magnitude of NVE is proportional to $1/T$ and to ground-state electronic energy differences due to isotopic substitutions.

Mass-independent fractionation (MIF).

Here we use Hg isotopes as an example to introduce the concept of mass-independent isotope fractionation (MIF). If we define $\delta^A Hg$ as

$$\delta^A Hg = [(^A Hg/^{198}Hg)_{sample}/(^A Hg/^{198}Hg)_{ref} - 1] \times 1000 \tag{6}$$

Then the mass-independent isotope fractionation (MIF) of any pair of Hg isotopes (e.g., $^A Hg/^{198}Hg$) will be

$$
\begin{aligned}
\Delta^A Hg &= \delta'^A Hg - \lambda_{MD}\delta'^{202}Hg \\
&= \lambda_{TOTAL}\delta'^{202}Hg - \lambda_{MD}\delta'^{202}Hg
\end{aligned} \tag{7}
$$

where $\delta'^{202}Hg = 1000 \cdot \ln\left(1 + \frac{\delta^{202}Hg}{1000}\right)$[51,52], λ_{TOTAL} includes λ_{MD} (the conventional mass-dependent scaling factor), λ_{NV} (the nuclear volume scaling factor), λ_{MIE} (the magnetic isotope effect scaling factor) and other scaling factors. And if we just consider the MIF caused by the NVE, it would be

$$\Delta_{NV}^A Hg = (\lambda_{NV} - \lambda_{MD})\delta'^{202}Hg \tag{8}$$

where λ_{MD} is actually calculated using the high temperature approximation of equilibrium fractionation[52]

$$\lambda_{\mathrm{MD}} = \frac{\left(\frac{1}{m_i} - \frac{1}{m_j}\right)}{\left(\frac{1}{m_i} - \frac{1}{m_k}\right)} \tag{9}$$

This is because λ_{MD} values for heavy metal isotope systems are only weakly temperature-dependent[53]. λ_{NV} is calculated from the mean square nuclear charge radii[4]

$$\lambda_{\mathrm{NV}} = \frac{<r_i^2> - <r_j^2>}{<r_i^2> - <r_k^2>} \tag{10}$$

where m_i, m_j and m_k are the masses of isotopes i, j and k, respectively; $<r_i^2>$, $<r_j^2>$ and $<r_k^2>$ are their mean square nuclear charge radii.

Unfortunately, $\Delta_{NV}^{A}\mathrm{Hg}$ cannot be calculated theoretically because the value of $\delta^{202}\mathrm{Hg}$ for a specific Hg species is unknown. Instead, we calculate the relative MIF in comparison of Hg vapor (Hg^0):

$$\Delta_{NV}^{A}\mathrm{Hg}_{\mathrm{HgX}} - \Delta_{NV}^{A}\mathrm{Hg}_{\mathrm{Hg}^0} = (\lambda_{NV}^{A} - \lambda_{MD}^{A}) \cdot 1000 \cdot \ln\ ^{202}\alpha_{\mathrm{HgX}-\mathrm{Hg}^0}^{NV} \tag{11}$$

If experimental results of MIF for Hg^0 vapor caused by NVE are available, we can obtain MIFs of other Hg species through "equation (11)". For example, Ghosh et al.[34] observed MIFs for odd isotopes ($^{199}\mathrm{Hg}$ and $^{201}\mathrm{Hg}$) and small MIFs for even isotope ($^{200}\mathrm{Hg}$) in the vapor phase (Hg^0) caused by NVE at room temperature. Their average $\Delta_{NV}^{199}\mathrm{Hg}$, $\Delta_{NV}^{201}\mathrm{Hg}$ and $\Delta_{NV}^{200}\mathrm{Hg}$ values for Hg^0 were $0.14 \pm 0.01\text{‰}$, $0.09 \pm 0.01\text{‰}$ and $0.01 \pm 0.03\text{‰}$, respectively. The results of equilibrium evaporation experiments of Estrade et al.[45] were similar to those of Ghosh et al.[34] and their $\Delta_{NV}^{199}\mathrm{Hg}$, $\Delta_{NV}^{201}\mathrm{Hg}$ and $\Delta_{NV}^{200}\mathrm{Hg}$ values for Hg^0 were 0.12‰, 0.07‰ and 0.01‰, respectively, in the temperature range of 2–22 °C.

Computational quantum chemistry methods. Ground-state electronic energies calculations are performed with DIRAC13.1 software package[54]. All-electron Dirac–Hartree–Fock (DHF) theory is used to calculate relativistic electronic structures of Hg-, Tl- and Pb-bearing species with four-component wave functions. Our calculation details are similar to those of Schauble[4]. "Double-zeta" basis sets[55,56] are used for Hg, Tl and Pb atoms and uncontracted cc-pVDZ basis sets[57] are used for other light atoms (H, O, C, Cl and Br). The molecular geometries were firstly optimized at pseudo-potential HF calculations (by Gaussian 03 software[58]) as initial guesses. Following the methods of Schauble[4], we optimize structures by using the iteratively quadratic fitting method (i.e., energy vs. bond-length fitting) instead of free geometry optimization using Dirac 13.1 to save computing time. $\mathrm{Hg(H_2O)_6^{2+}}$ (T_h), $\mathrm{HgCl_4^{2-}}$ (T_d), $\mathrm{Tl(H_2O)_6^{2+}}$ (T_h), $\mathrm{Tl(H_2O)_3^{+}}$ (C_3) and $\mathrm{PbCl_4^{2-}}$ (T_d) are chosen to compare their results calculated by the iteratively quadratic fitting method and by the free optimization method. The results show that these two methods can produce almost identical geometries but the former consumes much lesser time.

After geometry optimization, all Hg-, Tl- and Pb-bearing species are calculated for obtaining their ground-state electronic energies by using DIRAC 13.1. Different isotopologues will use their own Gaussian exponent ξ as in this form[59]:

$$\xi = \frac{3}{2<r^2>} \tag{12}$$

where the mean square nuclear charge radii ($<r^2>$) can be found from the Landolt-Boernstein Database[41] for Hg and from Angeli[42] for Tl and Pb.

Different from closed shell species, we also use the complete open shell configuration interaction (COSCI) method to calculate the ground-state energies of opened shell species (Tl^0 and Pb^0 with the electron configuration as $\mathrm{[Xe]4f^{14}5d^{10}6s^26p^1}$ and $\mathrm{[Xe]4f^{14}5d^{10}6s^26p^2}$, respectively).

With the calculated ground-state electronic energies, the NVE can be calculated from "equation (5)". For example, the NVE on isotope fractionation of an HgX-Hg^0 isotope exchange reaction is[4]

$$\begin{aligned}
1000 \cdot \ln\ \beta_{202-198}^{NV} &= 10^3\{-\Delta E_{202-198}[\mathrm{HgX-Hg^0}]\}/kT \\
&= 10^3\{(\mathrm{E}[^{202}\mathrm{Hg^0}] - \mathrm{E}[^{198}\mathrm{Hg^0}]) - (\mathrm{E}[^{202}\mathrm{HgX}] - \mathrm{E}[^{198}\mathrm{HgX}])\}/kT
\end{aligned} \tag{13}$$

where the $\beta(X)$ factor is the equilibrium fractionation factor between substance X and an ideal monoatomic gas[60].

The molecular geometries and harmonic interatomic vibrational frequency are calculated at pseudo-potential Hartree-Fock (HF) level by Guassian03 software package[58]. We treat inner-shell electrons of Hg, Tl, and Pb atom by using relativistic pseudo-potentials. However, valance and intermediate-shell electrons are treated with a double-zeta basis sets (cc-pVDZ–PP) and cc-pVDZ basis sets are used for H, C, O, Cl and Br atoms.

The usual isotope fractionation between substance A and substance B is defined as

40. Chen, J. B., Hintelmann, H., Feng, X. B. & Dimock, B. Unusual fractionation of both odd and even mercury isotopes in precipitation from Peterborough, ON, Canada. *Geochim. Cosmochim. Acta* **90,** 33–46 (2012).
41. Fricke, G. & Heilig, K. Group I: element particles, nuclei and atoms. Nuclear charge radii, Vol. **20,** 80-Hg mercury, 1-9 (Landolt-Brnstein: numerical data and functional relationships in Science and Technology, new series, 2004).
42. Angeli, I. A consistent set of nuclear rms charge radii: properties of the radius surface R (N, Z). *Atom. Data Nucl. Data Tables* **87,** 185–206 (2004).
43. Blum, J. D. & Bergquist. B. A. Reporting of variations in the natural isotopic composition of mercury. *Anal. Bioanal. Chem.* **388,** 353–359 (2007).
44. Ghosh, S., Xu, Y. F., Humayun, M. & Odom, L. Mass-independent fractionation of mercury isotopes in the environment. *Geochem. Geophys. Geosyst.* **9,** 1–10 (2008).
45. Estrade, N., Carignan, J., Sonke, J. E. & Donard, O. F. X. Mercury isotope fractionation during liquid-vapor evaporation experiments. *Geochim. Cosmochim. Acta* **73,** 2693–2711 (2009).
46. Smith, R. S. *et al.* Small-scale studies of roasted ore waste reveal extreme ranges of stable mercury isotope signatures. *Geochim. Cosmochim. Acta* **137,** 1–17 (2014).
47. Basu, A., Sanford, R. A., Johnson, T. M., Lundstrom, C. C. & Löffler, F. E. Uranium isotopic fractionation factors during U(VI) reduction by bacterial isolates. *Geochim. Cosmochim. Acta* **136,** 100–113 (2014).
48. Bopp, IV, C. J. *et al.* Uranium ^{238}U/^{235}U isotope ratios as indicators of reduction: results from an *in situ* biostimulation experiment at Rifle, Colorado, USA. *Environ. Sci. Technol.* **44,** 5927–5933(2010).
49. Kleinman, L. I. & Wolfsber, M. Corrections to Born-Oppenheimer approximation and electronic effects on isotopic-exchange equilibria. *J. Chem. Phys.* **59,** 2043–2053(1973).
50. Kleinman, L. I. & Wolfsber, M. Corrections to Born-Oppenheimer approximation and electronic effects on isotopic-exchange equilibria. 2. *J. Chem. Phys.* **60,** 4740–4748(1974).
51. Miller, M. F. Isotopic fractionation and the quantification of O-17 anomalies in the oxygen three-isotope system: an appraisal and geochemical significance. *Geochim. Cosmochim. Acta* **66,** 1881–1889 (2002).
52. Young, E. D., Galy, A. & Nagahara, H. Kinetic and equilibrium mass-dependent isotope fractionation laws in nature and their geochemical and cosmochemical significance. *Geochim. Cosmochim. Acta* **66,** 1095–1104 (2002).
53. Cao, X. B. & Liu, Y. Equilibrium mass-dependent fractionation relationships for triple oxygen isotopes. *Geochim. Cosmochim. Acta* **75,** 7435–7445 (2011).
54. Saue, T. *et al.* DIRAC, a program for atomic and molecular direct iterative relativistic all-electron calculations, release DIRAC13.1 (2013) Available at: http://dirac.chem.sdu.dk. (Acessed: 5th January 2014).
55. Dyall, K. G. Relativistic quadruple-zeta and revised triple-zeta and double-zeta basis sets for the 4p, 5p, and 6p elements. *Theor. Chem. Acc.* **115,** 441–447 (2006).
56. Dyall, K. G. & Gomes, A. S. P. Revised relativistic basis sets for the 5d elements Hf-Hg. *Theor. Chem. Acc.* **125,** 97–100 (2010).
57. Dunning, T. H. Gaussian-basis sets for use in correlated molecular calculations. 1. The atoms boron through neon and hydrogen. *J. Chem. Phys.* **90,** 1007–1023 (1989).
58. Frisch, M. J. *et al.* Gaussian software package, Inc., Pittsburgh PA. Gaussian 03, Revision B.04 (2003).
59. Visscher, L. & Dyall, K. G. Dirac–Fock atomic electronic structure calculations using different nuclear charge distributions. *Atom. Data Nucl. Data Tables* **67,** 207–224 (1997).
60. Richet, P., Bottinga, Y. & Javoy, M. Review of hydrogen, carbon, nitrogen, oxygen, sulfur, and chlorine stable isotope fractionation among gaseous molecules. *Ann. Rev. Earth Planet. Sci.* **5,** 65–110 (1977).

Acknowledgments

Author Contributions

Y.L. proposed and organized the project. S.Y. carried out the theoretical derivation and calculation work. S.Y. and Y.L. analyzed and interpreted the data together. S.Y. and Y.L. wrote the paper.

Additional Information

Supplementary information accompanies this paper at http://www.nature.com/srep

Competing financial interests: The authors declare no competing financial interests.

How to cite this article: Yang, S. and Liu, Y. Nuclear volume effects in equilibrium stable isotope fractionations of mercury, thallium and lead. *Sci. Rep.* **5,** 12626; doi: 10.1038/srep12626 (2015).